

the Hall voltage can come from the depletion layer,<sup>8</sup> since any carriers in that layer will have drift velocities comparable with those in the inversion layer and can be treated classically. At very low temperatures the number of such electrons is extremely small, and the considerations of Gurvich<sup>9</sup> may apply. The characteristic time for establishing a steady-state Hall voltage across the depletion layer is the dielectric relaxation time for the layer, which can be long enough to make possible an experimental separation of the slow depletion-layer contribution and the fast inversion-layer contribution.

At temperatures or inversion-layer concentrations high enough that more than one electronic subband is appreciably populated,<sup>10</sup> transfer of carriers between the subbands becomes important, and the simple considerations of this paper are no longer sufficient. Work is underway to extend the present results beyond the electric quantum limit, and to more general current, magnetic field, and surface orientations. When many subbands are occupied, the conventional theory<sup>1,2</sup> should be applicable.

I am grateful to S. Tansal and A. B. Fowler for many discussions of their experiments and their

relation to this work, and to R. S. Allgaier, M. H. Brodsky, W. E. Howard, G. Lasher, P. J. Price, and P. J. Stiles for helpful comments.

<sup>1</sup>E. H. Sondheimer, *Advan. Phys.* **1**, 1 (1952).

<sup>2</sup>D. K. C. MacDonald and K. Sarginson, *Proc. Roy. Soc. (London)*, Ser. A **203**, 223 (1950).

<sup>3</sup>F. Stern and W. E. Howard, *Phys. Rev.* **163**, 816 (1967).

<sup>4</sup>For example,  $\sum_{ij} z_{ni} z_{ij} z_{jn} = z_{nn}^3 - 2z_{nn}^2 z_{nn} + z_{nn}^3$ .

<sup>5</sup>The origin for the  $z$  coordinate is taken at the surface.

<sup>6</sup>W. A. Albers, Jr., and J. E. Thomas, Jr., *J. Phys. Chem. Solids* **14**, 181 (1960); W. A. Albers, Jr., *J. Phys. Chem. Solids* **23**, 1249 (1962).

<sup>7</sup>S. Tansal, A. B. Fowler, and R. F. Cotellera, *Bull. Am. Phys. Soc.* **13**, 1454 (1968), and *Phys. Rev.*, to be published. I am indebted to Mr. Tansal for a copy of this paper.

<sup>8</sup>The  $p$ -type bulk should not contribute to the Hall voltage when  $n$ -type contacts to the inversion layer are used, as in the work of Ref. 7. For results on a different parallel-layer structure, see M. H. Brodsky and R. B. Schoolar, to be published. I am indebted to Dr. Brodsky for a copy of this paper.

<sup>9</sup>Yu. A. Gurvich, *Fiz. Tek. Poluprov.* **1**, 1195 (1967) [translation: *Soviet Phys.—Semicond.* **1**, 999 (1968)].

<sup>10</sup>This applies to most of the results of Ref. 7.

## SPECTROSCOPIC DETERMINATION OF THE MAGNON DENSITY OF STATES OF $GdCl_3$ , A FERROMAGNETIC RARE-EARTH SALT\*

R. S. Meltzer, E. Cohen,† and H. W. Moos‡

Department of Physics, The Johns Hopkins University, Baltimore, Maryland

(Received 11 October 1968)

The magnon density of states of ferromagnetic  $GdCl_3$  in an external magnetic field has been observed by means of high-resolution optical spectroscopy. The relevant transitions arise from a single-ion transition mechanism, but the initial (magnon) and in some cases the final (exciton) states of the transitions are shown to have measurable dispersion, contrary to the usual description of rare-earth salts.

We have observed in the optical absorption spectrum of ferromagnetic  $GdCl_3$ , in an external magnetic field, transitions originating from a singly excited magnon whose line shapes are sufficiently resolved to yield information about the magnon density of states. To our knowledge, this is the first spectroscopic observation of the magnon dispersion of either a ferromagnet or a rare-earth salt. As a result, it is evident that high-resolution optical spectroscopy when used in conjunction with external magnetic fields can be useful in studying the magnon structure of materials with weak magnetic interactions.

In recent years magnons have been observed in

the optical spectra of several antiferromagnetic transition-metal compounds<sup>1</sup> for which the magnetic interactions are one to two orders of magnitude stronger than that of the rare earths. These transitions always involve an exchange-coupled mechanism in which the magnon and exciton are created or destroyed simultaneously on different sites of the crystal. They therefore appear as spin-assisted sidebands to the pure electronic transitions of the metallic ion. On the contrary, the transitions originating from a magnon state of  $GdCl_3$  arise from a single-ion transition mechanism. However, the excited states of the system can not always be classified simply as single-ion

Table 1. Properties of transitions from  ${}^8S_{7/2}$ ,  $M_J = \frac{5}{2}$  magnon state

Excited state	Polarization	Dominant dipole character <sup>a</sup>	$f_{\text{obs}}^b$ ( $\times 10^8$ )	$f_{\text{calc}}^c$ ( $\times 10^8$ )	$C(J, M_J, M_L, M_S = \frac{5}{2})$	Energy of observed density-of-state peaks
${}^6P_{7/2} \frac{7}{2}$	$\pi$	Magnetic	...	3.94	1	...
${}^6P_{7/2} \frac{5}{2}$	$\sigma$	Magnetic	7.0	7.03	2/7	0.6, 1.8
${}^6P_{7/2} \frac{3}{2}$	$\pi$	Magnetic	4.9	6.75	1/21	0.7, 2.0
${}^6P_{7/2} \frac{1}{2}$	$\sigma$	Electric	...	...	0	...
${}^6P_{5/2} \frac{5}{2}$	$\sigma$	Magnetic	3.2	1.87	5/7	0.4, 1.9
${}^6P_{5/2} \frac{3}{2}$	$\pi$	Magnetic	5.6	4.67	2/7	1.0, 2.0
${}^6P_{5/2} \frac{1}{2}$	$\sigma$	Electric	...	...	0	...

<sup>a</sup>In most cases we have only shown that the transition is predominantly of this dipole character.

<sup>b</sup> $f_{\text{obs}} = 1.09 \times 10^{-10} \int [\alpha(\bar{\nu}) / \langle n_{\Delta\bar{\nu}}^{\text{mag}} \rangle] d\bar{\nu}$  = observed oscillator strength.

<sup>c</sup> $f_{\text{calc}} = (8\pi^2 mc / \hbar e^2) \bar{\nu} |(-e/2mc) \langle \psi | \vec{L} + 2\vec{S} | \psi' \rangle|^2$  = calculated oscillator strength.

excitations as is usually done in the analysis of the optical spectrum of rare-earth salts since dispersion of both the magnetic excitation of the ground electronic state and of some of the excited electronic states appears evident.

We have obtained high-resolution ( $0.1 \text{ cm}^{-1}$ ) polarized absorption spectra of the transitions  ${}^8S_{7/2} \rightarrow {}^6P_{7/2}$ ,  ${}^6P_{5/2}$  at  $33000 \text{ cm}^{-1}$ . The spectra were studied photographically at  $1.45^\circ\text{K}$  as a function of external magnetic field oriented along the hexagonal axis of the crystal and photoelectrically at  $1.12$  and  $1.70^\circ\text{K}$  at a field of  $28.36 \text{ kG}$ . The photographs were made on a 5-m vacuum Ebert-Fastie spectrograph,<sup>2</sup> whereas the photoelectric traces were obtained on a 1.8-m spectrograph of the Ebert-Fastie design.<sup>3</sup> The axial spectrum was also obtained photoelectrically.

With no external magnetic field the transitions are broad and unresolved (half-width  $5\text{-}10 \text{ cm}^{-1}$ ). As the magnetic field is increased, the broad lines split into many transitions which become progressively sharper as the field is increased. At the maximum field of our experiments,  $36.5 \text{ kG}$ , only transitions from the  $M_J = \frac{7}{2}$  (ground) and  $M_J = \frac{5}{2}$  (magnon) components of the  ${}^8S_{7/2}$  state are sufficiently populated for observation. All transitions from the ground state which were not over-absorbed in our thinnest crystals ( $0.1 \text{ mm}$ ) have half-widths of less than  $0.2 \text{ cm}^{-1}$ , whereas the half-widths of all transitions from the magnon state were at least  $1 \text{ cm}^{-1}$ . The spectra appear to obey the selection rules of the  $C_{3h}$  site group of the hexagonal  $\text{GdCl}_3$  crystals,<sup>4</sup> i.e., magnetic dipole,  $\Delta M_J = 0(\sigma), \pm 1(\pi)$ ; electric dipole,  $\Delta M_J = \pm 2$  or  $\pm 4(\sigma), \pm 3(\pi)$ . The observed strengths of the magnetic dipole transitions are nearly identi-

cal to the calculated values as shown in Table I. That we observe single-ion selection rules and absorption strengths indicates that these are purely electronic single-ion transitions. The electric dipole strengths cannot be calculated a priori.

It should be noted that use of an external magnetic field in the study of the magnon state is advantageous and perhaps necessary for materials such as the rare-earth salts in which the magnetic effects are small. Firstly, the field separates in energy transitions from the ground and magnon states, making their observation easier. Secondly, the resulting depopulation of the magnon state causes a sharpening of the transitions as the magnetic field is increased.

At  $28.36 \text{ kG}$  we observe transitions which originate almost exclusively from the ground and single-magnon states. For the latter we find five magnetic dipole and two electric dipole transitions. These are listed in Table I. Only the magnetic dipole transitions are sufficiently separated from other transitions to give useful line shapes. Four of the five have almost identical shapes and energy separations from the equivalent transitions originating on the ground state. The line shape of a typical transition,  ${}^8S_{7/2}$ ,  $M_J = \frac{5}{2}$  to  ${}^6P_{7/2}$ ,  $M_J = \frac{3}{2}$ , is shown by the heavy solid curve in Fig. 1. The line shape of the exception, the transition  ${}^8S_{7/2}$ ,  $M_J = \frac{5}{2}$  to  ${}^6P_{7/2}$ ,  $M_J = \frac{7}{2}$ , is indicated by the long-short dashed curve.

The transitions originating from a magnon involve the destruction of the magnon and creation of an exciton. Since the pseudomomentum of the light wave is nearly zero, the wave vector of the exciton and magnon must be of the same magni-

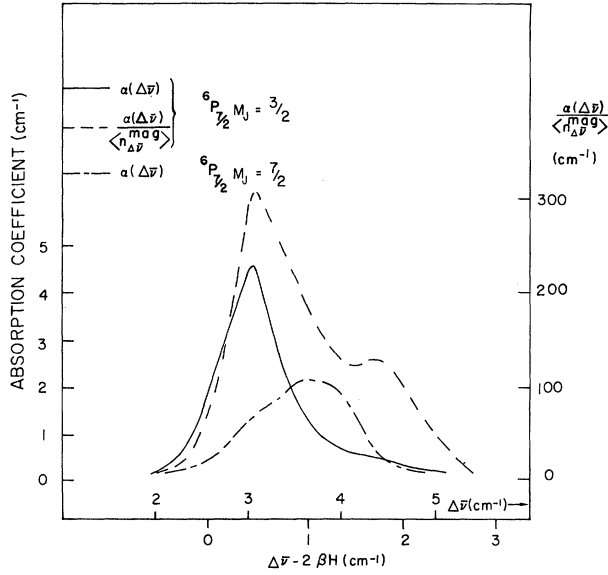


FIG. 1. Observed absorption coefficient and magnon density of states for the transitions  ${}^8S_{7/2}$ ,  $M_J = \frac{5}{2}$  to  ${}^6P_{7/2}$ ,  $M_J = \frac{3}{2}$  and  ${}^6P_{7/2}$ ,  $M_J = \frac{7}{2}$ . The scale on the left-hand side applies to the absorption coefficient  $\alpha(\bar{\nu})$ , that on the right-hand side to the magnon density of states  $\alpha(\bar{\nu})/\langle n_{\Delta\bar{\nu}}^{\text{mag}} \rangle$ . These spectra were obtained at 1.12°K with external magnetic field of 28.36 kG along the hexagonal axis. The upper scale of the abscissa measures the energy separation from the corresponding transition from the ground state, whereas the lower scale is this energy difference less the contribution to this splitting due to the external magnetic field.

tude but of opposite sign. The resulting line shape expression has the form

$$\alpha(\bar{\nu}) \sim |M_{ij}|^2 \sum_{\vec{k}} \langle n_{\vec{k}}^{\text{mag}} \rangle \times \delta(\bar{\nu} + \bar{\nu}_{\vec{k}}^{\text{mag}} - \bar{\nu}_{-\vec{k}}^{\text{ex}}), \quad (1)$$

where  $\alpha(\bar{\nu})$  is the absorption coefficient,  $M_{ij}$  is the single-ion transition moment between states  $i$  and  $j$ ,  $\langle n_{\vec{k}}^{\text{mag}} \rangle$  is the magnon occupation number,  $\bar{\nu}_{\vec{k}}^{\text{mag}}$  and  $\bar{\nu}_{-\vec{k}}^{\text{ex}}$  are the magnon and exciton dispersion energies, respectively, and  $\bar{\nu}$  is the photon energy. Unlike the corresponding expression for magnon sidebands, all points in  $\vec{k}$  space are equally weighted since the transition moment is independent of  $\vec{k}$ .

If the exciton has no dispersion, then the spectroscopically observed energy difference  $\Delta\bar{\nu}$  between a transition from the ground state and a corresponding transition from the magnon state is just the magnon dispersion. Under this circumstance,  $\langle n_{\vec{k}}^{\text{mag}} \rangle$  is a function only of  $\Delta\bar{\nu}$  and

can be removed from the summation of Eq. (1). We may then write

$$\alpha(\bar{\nu})/\langle n_{\Delta\bar{\nu}}^{\text{mag}} \rangle \sim \sum_{\vec{k}} \delta(-\Delta\bar{\nu} + \bar{\nu}_{\vec{k}}^{\text{mag}}), \quad (2)$$

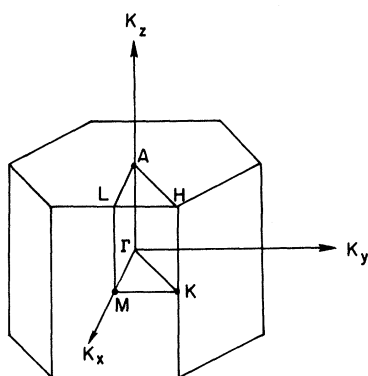
which is simply the density of states for the magnon as a function of energy above the ground state.

We believe that the four transitions with similar line shapes involve excited states with small (less than  $0.5 \text{ cm}^{-1}$ ) exciton dispersion, whereas the transition to the  ${}^6P_{7/2}$ ,  $M_J = \frac{7}{2}$  state shows measureable (more than  $0.5 \text{ cm}^{-1}$ ) exciton dispersion. The exchange matrix elements responsible for the exciton dispersion involve the exchange of two electrons with the resulting exchange of the excitation between two neighboring ions. A two-electron exchange (spin-independent operator) cannot result in the exchange of more than one unit of spin projection between the two ions. Since the ground state is  $M_S = \frac{7}{2}$ , the excited state must contain some  $M_S = \frac{5}{2}$  character if dispersion is to occur; i.e., we must determine the coupling coefficients  $C(J, M_J, M_L, M_S = \frac{5}{2})$  of the expansion

$$|{}^6P_{J, M_J}\rangle = C(J, M_J, M_L, M_S = \frac{5}{2}) \times |{}^6P, M_L, M_S\rangle. \quad (3)$$

The square of the coefficients which appear in the relevant exchange matrix elements are listed in Table I. Other things being equal, the  ${}^6P_{7/2}$ ,  $M_J = \frac{7}{2}$  exciton should have the largest dispersion, the dispersion decreasing for lower values of  $M_J$ .

Furthermore, if one assumes no exciton dispersion for these four excited states, one can correlate the energy features of the resulting density-of-states curve  $\alpha(\bar{\nu})/n_{\Delta\bar{\nu}}^{\text{mag}}$  with the energy of those points of the first Brillouin zone with a high density of states, as calculated for  $\text{GdCl}_3$  by Marquard and Stinchcombe.<sup>5</sup> These calculations, based upon the exchange parameters obtained from thermodynamic data,<sup>6</sup> indicate two possible pairs of nearest- and next-nearest-neighbor exchange parameters. The resulting magnon dispersions have two branches, an optical and an acoustical mode. Transitions from both occur in the optical spectrum. The first Brillouin zone of  $\text{GdCl}_3$ , with its points of high symmetry labeled, is shown in Fig. 2. Peaks in the density of states are likely near the  $A$  and  $M$  points of the zone. The magnon energies for points  $A$  and  $M$  calculated for the exchange

FIG. 2. First Brillouin zone for  $\text{GdCl}_3$ .

parameters of set A ( $J_1 = 0.051 \text{ cm}^{-1}$ ,  $J_2 = 0.005 \text{ cm}^{-1}$ ) are 1.92 and  $0.96 \text{ cm}^{-1}$ , respectively, for the optical modes, and  $1.92$  and  $0.68 \text{ cm}^{-1}$  for the acoustic modes. For set B ( $J_1 = -0.016 \text{ cm}^{-1}$ ,  $J_2 = 0.029 \text{ cm}^{-1}$ ) the energies are 0.97, 2.22, and  $0.97, 1.38 \text{ cm}^{-1}$ , in the same order. The spectroscopically observed density-of-states curve obtained from Eq. (2) for the transition to the  ${}^6P_{7/2}$ ,  $M_J = \frac{3}{2}$  state is shown by the dashed curve in Fig. 1. It has two peaks as do the curves from all four of the nearly identical line shapes. The energies of these peaks relative to the corresponding transitions from the ground state, less the contribution to the splitting of the ground and magnon state from the external magnetic field, are listed in the last column of Table I.<sup>7</sup> These values are very close to those calculated for the A and M points.

It the above analysis is correct, the overall breadths of the line shapes favor the parameters of set B as the total spread of the magnon dispersion for set A is only  $1.65 \text{ cm}^{-1}$ , whereas for set B it is  $2.72 \text{ cm}^{-1}$ . In addition, the calculated magnon dispersions for both set A and set B suggest that the greatest density of states lies at the top surface of the zone over which the dispersion is nearly flat. We observe the greatest density of states at an energy of about  $0.8 \text{ cm}^{-1}$ . This is almost identical to the energy of the A point for set B ( $0.97 \text{ cm}^{-1}$ ), but not that of set A ( $1.92$

$\text{cm}^{-1}$ ). A complete calculation of the density of states based upon these two sets of parameters is necessary to settle this question, but it should be noted that the parameters of set B are supported by an analysis of the EPR spectrum of  $\text{Gd}^{+3}$  pairs in  $\text{LaCl}_3$  and  $\text{EuCl}_3$ .<sup>8</sup>

We are presently studying the line shapes as a function of temperature, both in absorption and emission, in order to examine the exciton dispersion in the several states more carefully. We are also examining some weak absorption lines, not identifiable with single-ion transitions, whose position and magnetic field splitting suggest a transition in which both an exciton and magnon are simultaneously created. The results of this work and a more comprehensive discussion of the spectrum will be presented elsewhere.

---

\*Partially supported by the National Aeronautics and Space Administration and the U. S. Army Research Office, Durham, N. C.

†Present address: Bell Telephone Laboratories, Murray Hill, N. J.

‡Alfred P. Sloan Foundation Fellow.

<sup>1</sup>A review article on the subject through 1967 is given by D. D. Sell, *J. Appl. Phys.* **39**, 1030 (1968).

<sup>2</sup>H. M. Crosswhite and H. W. Moos, in *Optical Properties of Ions in Crystals*, edited by H. M. Crosswhite and H. W. Moos (Interscience Publishers, Inc., New York, 1967), p. 3.

<sup>3</sup>W. G. Fastie, H. M. Crosswhite, and P. Gloersen, *J. Opt. Soc. Am.* **48**, 106 (1958).

<sup>4</sup>W. H. Zachariasen, *J. Chem. Phys.* **16**, 254 (1948).

<sup>5</sup>C. D. Marquard and R. B. Stinchcombe, *Proc. Phys. Soc.* **92**, 665 (1967).

<sup>6</sup>C. D. Marquard, *Proc. Phys. Soc.* **92**, 650 (1967).

<sup>7</sup>Here we have assumed that the whole magnon dispersion is uniformly shifted in energy by an external magnetic field. Marquard and Stinchcombe have shown, however, that the spin reversal associated with the magnon is not always unity so that the resulting energy shift is  $\vec{k}$  dependent, particularly for the acoustic modes near the center and basal plane of the zone. It must therefore be remembered that the density of states may depend somewhat on the external magnetic field.

<sup>8</sup>R. J. Birgeneau, M. T. Hutchings, and W. P. Wolf, *J. Appl. Phys.* **38**, 957 (1967).